



# HHS Public Access

Author manuscript

*Arch Pathol Lab Med.* Author manuscript; available in PMC 2024 November 07.

Published in final edited form as:

*Arch Pathol Lab Med.* 2024 March 01; 148(3): 327–335. doi:10.5858/arpa.2022-0427-OA.

## Characterizing Lung Particulates Using Quantitative Microscopy in Coal Miners With Severe Pneumoconiosis

**Jeremy T. Hua, MD,**

Division of Environmental and Occupational Health Sciences, National Jewish Health, Denver, Colorado; Division of Pulmonary Sciences and Critical Care Medicine, University of Colorado, Aurora; Department of Epidemiology in the Colorado School of Public Health, University of Colorado, Aurora

**Carlyne D. Cool, MD,**

Division of Pathology, National Jewish Health, Denver, Colorado; Department of Pathology, University of Colorado, Aurora

**Heather A. Lowers, MS,**

Geology, Geophysics, and Geochemistry Science Center, US Geological Survey, Denver, Colorado

**Leonard H. T. Go, MD,**

Environmental and Occupational Health Sciences Division, University of Illinois Chicago School of Public Health, Chicago

**Lauren M. Zell-Baran, MPH,**

Division of Environmental and Occupational Health Sciences, National Jewish Health, Denver, Colorado; Department of Epidemiology in the Colorado School of Public Health, University of Colorado, Aurora

**Emily A. Sarver, PhD, MS,**

Department of Mining and Minerals Engineering, Virginia Tech, Blacksburg

**Kirsten S. Almberg, PhD, MS,**

Environmental and Occupational Health Sciences Division, University of Illinois Chicago School of Public Health, Chicago

**Kathy D. Pang, MPH,**

Division of Environmental and Occupational Health Sciences, National Jewish Health, Denver, Colorado

**Susan M. Majka, PhD,**

---

Any use of trade, firm, or product names is for descriptive purposes only and does not imply endorsement by the US government.

Corresponding author: Jeremy T. Hua, MD, Division of Environmental and Occupational Health Sciences, National Jewish Health, 1400 Jackson St, Denver, CO 80206 (hua.j@njhealth.org).  
Cohen and Rose are co-senior authors.

Go provides expert witness testimony in workers' compensation cases. The other authors have no relevant financial interest in the products or companies described in this article.

Some of the results of this study were previously reported in the form of an abstract/poster at the American Thoracic Society International Conference; May 16, 2022; San Francisco, California.

Division of Pulmonary, Critical Care, and Sleep Medicine, National Jewish Health, Denver, Colorado

**Angela D. Franko, MD,**

Department of Pathology and Laboratory Medicine, University of Calgary, Calgary, Alberta, Canada

**Naseema I. Vorajee, MD,**

Department of Histopathology, Lancet Laboratories, Johannesburg, South Africa

**Robert A. Cohen, MD,**

Environmental and Occupational Health Sciences Division, University of Illinois Chicago School of Public Health, Chicago

**Cecile S. Rose, MD, MPH**

Division of Environmental and Occupational Health Sciences, National Jewish Health, Denver, Colorado; Division of Pulmonary Sciences and Critical Care Medicine, University of Colorado, Aurora

## Abstract

**Context.**—Current approaches for characterizing retained lung dust using pathologists' qualitative assessment or scanning electron microscopy with energy-dispersive spectroscopy (SEM/EDS) have limitations.

**Objective.**—To explore polarized light microscopy coupled with image-processing software, termed quantitative microscopy–particulate matter (QM-PM), as a tool to characterize in situ dust in lung tissue of US coal miners with progressive massive fibrosis.

**Design.**—We developed a standardized protocol using microscopy images to characterize the in situ burden of birefringent crystalline silica/silicate particles (mineral density) and carbonaceous particles (pigment fraction). Mineral density and pigment fraction were compared with pathologists' qualitative assessments and SEM/EDS analyses. Particle features were compared between historical (born before 1930) and contemporary coal miners, who likely had different exposures following changes in mining technology.

**Results.**—Lung tissue samples from 85 coal miners (62 historical and 23 contemporary) and 10 healthy controls were analyzed using QM-PM. Mineral density and pigment fraction measurements with QM-PM were comparable to consensus pathologists' scoring and SEM/EDS analyses. Contemporary miners had greater mineral density than historical miners (186 456 versus 63 727/mm<sup>3</sup>;  $P = .02$ ) and controls (4542/mm<sup>3</sup>), consistent with higher amounts of silica/silicate dust. Contemporary and historical miners had similar particle sizes (median area, 1.00 versus 1.14  $\mu\text{m}^2$ ;  $P = .46$ ) and birefringence under polarized light (median grayscale brightness: 80.9 versus 87.6;  $P = .29$ ).

**Conclusions.**—QM-PM reliably characterizes in situ silica/silicate and carbonaceous particles in a reproducible, automated, accessible, and time/cost/labor-efficient manner, and shows promise as a tool for understanding occupational lung pathology and targeting exposure controls.

Analysis of lung histopathology and retained dust particulate may improve diagnostic accuracy and exposure assessment in patients with occupational lung disease, especially when workplace exposure measurements are limited. For example, a multimodal approach using pulmonary pathologist evaluation and scanning electron microscopy with energy-dispersive spectroscopy (SEM/EDS) of lung tissue recently implicated respirable crystalline silica (RCS) exposure in the resurgence of severe coal workers' pneumoconiosis in contemporary US coal miners born after 1930, particularly those working in central Appalachia.<sup>1</sup>

Current histopathologic techniques for evaluating lung tissue particulate matter in work-related lung diseases have limitations. Specialized training is required for pulmonary pathologists' qualitative assessments, and interrater agreement for pathologists' scoring has been found to vary widely.<sup>2</sup> Efforts to develop consensus interpretations among multiple pulmonary pathologists are labor-intensive. Indeed, we found that approximately 2000 hours were required to obtain independent assessments from a 7-member pulmonary pathologist panel and achieve consensus for multiple discordant histopathologic variables characterizing pneumoconiosis in US coal miners.<sup>1</sup> SEM/EDS characterizes dust particle elemental composition but requires advanced training and specialized equipment and is also labor-intensive. Tissue digestion is sometimes required to extract particulate matter for SEM/EDS particle analyses, adding further complexity and variability.

RCS and other silicates are often the most abundant minerals in respirable coal mine dust.<sup>3</sup> They also exhibit birefringence under cross-polarized light microscopy (PLM), allowing for visualization of particles in lung tissue against a darkly contrasted background.<sup>4-6</sup> Modern conventional light microscopes allow high-resolution digital microscopy images to be obtained, and automated image postprocessing algorithms enable identification of histopathologic features such as fluorescent tissue markers.<sup>7</sup> Recent PLM developments have shown promise for counting and differentiating dust particles, including coal, carbonates, silica, and silicates in environmental samples.<sup>8</sup> However, to our knowledge, quantitative techniques for characterizing in situ dust particles in lung tissue using PLM have not been developed.

In addition to birefringent particles consistent with RCS and silicates, anthracotic pigment in lung tissue accumulates from inhalation of carbonaceous particles, such as coal dust, combustion products, and cigarette smoke.<sup>9</sup> Coal macules and nodules have characteristic darkly pigmented areas under bright-field microscopy.<sup>6</sup> Accurate quantification and characterization of in situ particulate matter (both birefringent particles and pigmented materials) has the potential to inform clinical diagnosis of exposure-related lung diseases, prognosis, future medical screening, and workplace exposure control regulations.

We explored a novel application of quantitative microscopy with automated image-processing algorithms in lung tissue from coal miners with dust-related disease, termed quantitative microscopy-particulate matter (QM-PM), to characterize in situ carbonaceous particles, silica, and silicates. We assessed the reliability of this technique using lung tissue samples obtained from US coal miners with progressive massive fibrosis (PMF), the most severe form of pneumoconiosis, that previously were demographically and

histopathologically well characterized.<sup>1</sup> We sought to determine if QM-PM measurements could reproduce previous findings that contemporary miners born after 1930, who most likely worked with mechanized mining equipment, have greater lung tissue burden of birefringent particles consistent with RCS and silicates compared with historical miners. We also hypothesized that our QM-PM findings would be comparable to pathologists' qualitative consensus scores and SEM/EDS results.

## METHODS

### Tissue Sample Acquisition

We obtained hematoxylin-eosin (H&E)-stained samples (5- $\mu$ m thickness) for QM-PM analysis from a recently published study by Cohen et al<sup>1</sup> of US coal miners with PMF.<sup>1</sup> PMF was defined in that study as a dust-related fibrotic lesion measuring greater than 1 cm in longest dimension with irregular or whorled collagen fibers, with or without necrotic areas, and presence of dust consistent with coal mine dust. Sample selection and inclusion methods are described in Cohen et al.<sup>1</sup> This study was approved by the Biomedical Research Alliance of New York (Lake Success, New York) institutional review board (#HS-3039-528). Birth year after 1930 was used as a surrogate for contemporary coal miners working primarily during an era of highly mechanized mining in the United States, using equipment and practices that are thought to have indirectly increased exposure to RCS and silicates from rock strata above, below, and within the coal seam.

We also obtained H&E-stained control lung tissue samples from deceased individuals without known lung disease banked at National Jewish Health (Denver, Colorado) at the time of organ donation. Available demographic information for controls was reported by next of kin and included age, sex, current/former cigarette smoking status, and pack-year smoking history.

### Tissue Area Measurement

We obtained bright-field microscopy images of H&E-stained lung tissue slides, scanned at  $\times 40$  magnification, using Aperio XT (Software ImageScope v8.2, Leica Biosystems, Buffalo Grove, Illinois). Images were downloaded at  $4.0 \times 4.0 \mu\text{m}/\text{pixel}$  resolution and are referred to as the bright-field reference. We used ImageJ v1.53 software (National Institutes of Health, Bethesda, Maryland)<sup>10</sup> and the Bio-Formats plugin to generate a binary image based on the bright-field reference, such that grayscale pixels (range, 0 [black]–255 [white]) darker than the background glass microscope slide were identified as tissue. The binary image was used to calculate total tissue area (in square micrometers), and total tissue volume after multiplying by tissue slice thickness (Figure 1, A and C).

For each tissue specimen, we also analyzed an area of interest consisting of the PMF lesion(s) and compared it with the surrounding non-PMF region. An expert pathologist demarcated the PMF-specific tissue area using the freehand trace tool in ImageJ (Figure 1, B and D).

## Pigmented (Coal/Carbonaceous) Particle Characterization

Automated identification of pigmented regions was performed in ImageJ by using the bright-field reference image. We optimized a brightness threshold (pixel brightness under red channel spectrum  $<100$ ) and set it to identify brown-black pixels darker than surrounding tissue as pigmented regions (Figure 2, A through D). The pigment fraction for the whole tissue sample or for the area of interest was calculated by dividing the pigmented area by the entire tissue area or area of interest, respectively.

## Birefringent Mineral Particle Characterization

**PLM Image Acquisition.**—PLM images were obtained at  $\times 20$  magnification, 1/7.5-second exposure time, and  $0.38 \times 0.38 \mu\text{m}$ / pixel resolution and autofocused along a single horizontal z-plane using a conventional light microscope, Keyence BZ-X810 (Keyence Corporation, Osaka, Japan), with a Jigtech N11599 polarizer lens and filter cube (Daitron Incorporated, Wilsonville, Oregon). Microscope, polarizer, and camera settings were optimized and remained consistent for all samples. Edge points were manually assigned along tissue borders. The number of images obtained per sample ranged from 1000 to 4000 depending on tissue sample size.

**Birefringent Particle Identification and Characterization.**—We used the built-in Keyence BZ-X800 software with the automated Macro Hybrid Cell Count feature to identify birefringent particles from PLM images, which were expected to consist primarily of RCS and silicates.<sup>5</sup> Overlay images were created for each sample by setting a grayscale pixel threshold above which birefringent particles appeared illuminated under PLM as compared with the background tissue. We visually inspected approximately 10 selected images per sample to optimize the threshold that most effectively captured birefringent particles and excluded collagen fibers that appeared tan-orange under PLM (Figure 3, A through C).<sup>11</sup> An upper size limit for particles of  $50 \mu\text{m}^2$  was used to exclude regions likely to be artifact. Individual particle area and long- and short-axis dimensions were measured. Mean particle grayscale brightness, a value between 0 for black and 255 for white, was measured and was a surrogate for the degree of birefringence. Silicates are expected to appear brighter and be strongly birefringent, whereas RCS appears more weakly birefringent.<sup>4</sup> We then implemented this protocol across all 1000 to 4000 images per sample in an automated manner. The smallest identifiable particle was approximately  $0.3 \mu\text{m}$  in short-axis dimension and  $0.4 \mu\text{m}^2$  in area.

We calculated the total birefringent mineral particle count across an entire sample. We defined the density of birefringent mineral particles, referred to as mineral density, as the total birefringent mineral particle count divided by the tissue volume. The cumulative birefringent mineral particle area was the sum of the area of all identified birefringent particles in square micrometers. The Mineral:Carbon<sub>[QM]</sub> ratio was calculated as the ratio of birefringent mineral particle area to total pigmented area for each sample. These steps were repeated for the exclusive PMF and non-PMF tissue regions.

## Quantitative Microscopy Versus Qualitative Pathologist Comparison Variables

**Pathologist Consensus Classification.**—Coal miner samples were previously evaluated by 5 pulmonary pathologist teams and visually scored for type of PMF, using definitions of 25% or less (coal type), more than 75% (silica type), and more than 25% and less than 75% (mixed type) based on estimated percentage of the PMF lesions containing silicotic nodules.<sup>1</sup> Samples were also scored by pathology teams for qualitative birefringent particle profusion (mild, moderate, or severe) based on visual appearance under PLM using reference images agreed upon prior to review. Discordant classifications, defined as any disagreement on type of PMF or qualitative birefringent particle profusion, were resolved by consensus involving all study pathologists.

We examined whether mineral density and Mineral:Carbon<sub>[QM]</sub> ratio correlated with the pathologists' qualitative score for birefringent particle profusion. We also analyzed whether coal-type PMF lesions would have greater pigment fraction measured using QM-PM compared with mixed-type PMF, and whether both would have greater pigment fraction than silica-type PMF.

**SEM/EDS Measurements.**—Tissue digestion was performed on a subset of samples for SEM/EDS evaluation of particle chemical composition. Approximately 1000 to 2000 particles were analyzed per sample, and concentrations of silica, silicate, and carbonaceous particles were estimated. An overview of tissue digestion methods to collect particulate matter for characterization by SEM/EDS is described elsewhere.<sup>12</sup> However, adjustments to those methods were needed, as the particle loads in lung tissue samples examined in this study were greater than those examined in Lowers et al.<sup>12</sup> Specific changes included (1) using 20-mm formalin-fixed, paraffin-embedded tissue scrolls rather than 60- to 100-mm scrolls; (2) transferring dried tissue to 25 mL of bleach and reacting for 2 hours; (3) filtering the suspension through a 25-mm-diameter, 0.1-mm-track etch polycarbonate filter; (4) excluding particles less than 0.1  $\mu\text{m}$  in longest dimension; and (5) setting stopping criteria to 2000 particles or 110 fields of view. The automated particle analysis was performed on an FEI field emission scanning electron microscope (FEI Company, Hillsboro, Oregon) operated at 15 kV, spot size 5, working distance of 11 mm, 30- $\mu\text{m}$  objective aperture, and magnification set to  $\times 3000$  for a 48-mm-wide field of view.

Automated particle information was collected using the Feature module of the Oxford Instruments Aztec Analysis Software suite (Oxford Instruments, Oxfordshire, England). Particle selection thresholds were calibrated to ignore the polycarbonate filter and select all pixels brighter than the filter on backscattered electron images. Energy-dispersive spectra were acquired for 5 seconds per feature with an Oxford Instruments X-Max 50 mm<sup>2</sup> silicon drift detector. The particle classification, area, long and short axis dimensions, breadth, length, and perimeter were recorded in a table.<sup>13</sup> Specific constituents were normalized to the volume of tissue (cubic millimeters).

The summed concentration of silica and silicate particles using SEM/EDS divided by the concentration of carbonaceous particles represented the Mineral:Carbon<sub>[SEM/EDS]</sub> ratio. These values were compared with the measured Mineral:Carbon<sub>[QM]</sub> ratio.

## Statistical Analyses

All data management and analyses were performed in R v4.1.2 (R Foundation for Statistical Computing, Vienna, Austria). Particle size and brightness are presented as median (25th–75th percentile), and other summary statistics are presented as mean  $\pm$  SD. Two-tailed *t* tests were used for comparison, of sample-level variables. One-way analysis of variance was used for group comparison, with the post-hoc Tukey test for multiple pairwise comparisons. Particle size and brightness were compared with linear mixed models, using groups as fixed effects and samples as random effects. In order to meet test assumptions, nonnormally distributed measurements were log transformed before analysis. *P* values of less than .05 were considered statistically significant. The Mineral:Carbon ratios measured via SEM/EDS and QM-PM were compared using the Pearson correlation coefficient (*r*). Correlation was interpreted as 0.00 to 0.09, negligible; 0.10 to 0.39, weak; 0.40 to 0.69, moderate; 0.70 to 0.89, strong; and 0.90 to 1.00, very strong.<sup>14</sup>

## RESULTS

We used QM-PM to analyze lung tissue samples from 10 controls and 62 historical and 23 contemporary US coal miners with PMF. Table 1 shows participants' demographic data, work tenure, smoking history, and work in a central Appalachian state, and also the distribution of pathologist consensus groups. Additional demographic information is described in a separate report.<sup>1</sup>

The mean number of birefringent particles identified among coal miners with PMF was  $113\,284 \pm 186\,678$ , compared with  $210 \pm 158$  for control subjects. Mineral particle size was smaller in miners than in controls (median area, 1.00 versus  $1.57\ \mu\text{m}^2$ ;  $P < .001$ ). Mean particle grayscale brightness (range, 0 [black]–255 [white]), a measure associated with mineral particle type, was  $92.1 \pm 31.9$  in miners, compared with  $160.1 \pm 36.6$  ( $P < .001$ ) in controls. Mineral particles in contemporary and historical miners were similar in median area (1.00 versus  $1.14\ \mu\text{m}^2$ ;  $P = .46$ ) and brightness (80.9 versus 87.6;  $P = .29$ ). Additional particle-level details are shown in Table 2. Cumulative frequencies of particle area and grayscale brightness by miner birth cohort are shown in Figure 4, A and B.

Mineral density using QM-PM for all miners was  $96\,936 \pm 140\,008$  birefringent particles/ $\text{mm}^3$  tissue (range, 2342–824 422/ $\text{mm}^3$ ), significantly greater than for control subjects ( $4542 \pm 4543/\text{mm}^3$ ;  $P < .001$ ). Notably, mineral density in contemporary miners was significantly greater than in historical miners ( $186\,456 \pm 234\,253$  versus  $63\,727 \pm 55\,318/\text{mm}^3$ ;  $P = .02$ ). The measured Mineral:Carbon<sub>[QM]</sub> ratio was also significantly greater in miners compared with control subjects (0.49 versus 0.19;  $P = .04$ ), and contemporary miners had greater Mineral:Carbon<sub>[QM]</sub> ratio than historical miners (1.21 versus 0.23;  $P = .002$ ) (Table 2).

Mineral density using QM-PM correlated with qualitative birefringent particle profusion, increasing successively from mild ( $37\,372 \pm 42\,259/\mu\text{m}^3$ ) to moderate ( $91\,865 \pm 111\,806/\text{mm}^3$ ) to severe ( $206\,976 \pm 224\,253/\mu\text{m}^3$ ) (analysis of variance  $P < .001$ ;  $P < .05$  in pairwise Tukey test), which were all significantly greater than mineral density in controls.

A similar association was observed between the Mineral:Carbon<sub>[QM]</sub> ratio and profusion category (Table 2).

Pigment fraction using QM-PM was not significantly different among control samples ( $0.19\% \pm 0.14\%$ ), silica-type PMF lesions ( $0.28\% \pm 0.27\%$ ), and mixed-type PMF lesions ( $0.49\% \pm 0.36\%$ ). However, pigment fraction was substantially greater in coal-type PMF ( $1.05\% \pm 0.65\%$ ;  $P < .05$  in pairwise Tukey test) compared with all other groups.

We also analyzed pigment fraction, mineral density, and Mineral:Carbon<sub>[QM]</sub> in the PMF-only areas of interest. These results showed the same group-level patterns seen in the whole-sample analyses (data not shown). PMF lesions occupied a mean of  $52.6\% \pm 24.1\%$  (range, 5.5%–100%) of the whole tissue regions. PMF lesions showed a greater mean pigment fraction than exclusive non-PMF areas ( $0.8\% \pm 0.7\%$  versus  $0.5\% \pm 0.5\%$ ;  $P = .005$ ), but mineral density was similar ( $94\,198 \pm 146\,033$  versus  $101\,275 \pm 144\,081$ ;  $P = .80$ ).

Particle birefringence for every mineral particle identified using QM-PM in all samples was grouped by particle size to assess whether particle birefringence might be technically limited by small particle size (Figure 5). Mean particle birefringence increased with larger particle size, though, notably, strong birefringence (brightness values closer to 255) was observed even in the smallest mineral particles ( $<0.5\ \mu\text{m}^2$ ). SEM/EDS analyses were available for 65 of 85 miners. There was moderate correlation between measured Mineral:Carbon<sub>[QM]</sub> and Mineral:Carbon<sub>[SEM/EDS]</sub> ( $r = 0.52$ ,  $P < .001$ ).

## DISCUSSION

Findings from this study reflect the first known effort to quantitatively characterize in situ dust particulate matter in lung tissue using conventional PLM. We demonstrated that QM-PM characteristics of birefringent RCS, silicates, and pigmented carbonaceous particles were comparable to findings from pathologist qualitative assessments. Birefringent mineral density using QM-PM successively increased among mild, moderate, and severe birefringent profusion groups by pathologist consensus, and all were greater than measured mineral density in normal controls. The pigment fraction was greatest in samples classified by pathologists as coal-type PMF lesions, compared with mixed-type and silica-type lesions. We found moderate correlation between Mineral:Carbon ratios measured by QM-PM and SEM/EDS. These findings suggest that QM, with algorithmic identification of RCS, silicates, and carbonaceous dust, may be a reliable addition to expert pathologists' qualitative assessment and SEM/EDS.

Contemporary US coal miners have suffered a resurgence of the most severe form of pneumoconiosis in recent decades.<sup>1,15</sup> Our findings add support to previous work implicating silica derived from rock strata above, below, and within coal seams as playing an important role.<sup>1</sup> A greater concentration of birefringent particles, presumably RCS and other silicates, was measured in contemporary coal miners compared with historical coal miners. Mineral particles in contemporary and historical miners had similar brightness under PLM, though a nonsignificant trend toward weaker birefringence in contemporary miners

may suggest even greater exposure to RCS than to silicates (80.9 versus 87.6;  $P = .29$ ). Recent analysis of these same tissue samples showed a greater percentage and concentration of silica particles in contemporary miners using SEM/EDS.<sup>1</sup> Mineral particle size was comparable between contemporary and historical miners and was significantly smaller than in controls, findings that cannot be reliably characterized by pathologist evaluation.

QM-PM has a number of advantages over existing techniques for characterizing and quantifying lung particulate matter. The methodology involves approximately 4 to 8 total hours per tissue sample, substantially less time than pathologists' assessment with consensus meetings. Most of this period consists of passive microscope and computer processing time without active operator input, and many steps may be performed overnight for multiple samples. In contrast, evaluation of particulate matter by in situ SEM/EDS is time-consuming and limited to a small subset of particles within a sample. Sampling bias inherent to in situ SEM/EDS, where particles are manually selected for counting, is eliminated with QM-PM, where the entire sample is analyzed. QM-PM is fully automated other than identifying tissue sample edges and tracing regions of interest, and could be performed by a technician with minimal clinical/technical training. Imaging parameters and particle-identifying thresholds were optimized during pilot testing and were implemented reproducibly in all study samples. This is in contrast to less reliable interrater classifications of specimens inherent to subjective qualitative measures. Additionally, the use of a conventional light microscope, polarizing lens, and open-access image-processing software is substantially less costly than evaluation by expert pulmonary pathologists or SEM/EDS, and digestion or destruction of lung tissue is not necessary, unlike for some SEM/EDS protocols.

We used mean grayscale brightness as an indicator of RCS burden. Previous work has described differences in relative brightness among distinct mineral types viewed by pathologists under PLM, including the dull (weakly birefringent) appearance of RCS and substantially brighter (strongly birefringent) appearance of silicates.<sup>4-6</sup> However, accurate differentiation of RCS from silicates under PLM is challenged by several technical factors, including particle agglomeration, interactions with surrounding lung tissue, and potential differences in birefringent properties that have not yet been investigated in respirable-sized particles. Santa et al<sup>8</sup> deployed PLM to differentiate coal from mineral particles in composite dust samples, but quantitative comparisons between distinct mineral particle types using PLM have yet to be performed. Additional uncertainty may be introduced from coated particles, such as aluminosilicate-occluded silica particles previously reported in coal mine dust,<sup>16,17</sup> but distinguishing these particles under PLM needs further exploration. QM-PM characterization of retained mineral particles, including RCS, silicates, and other birefringent minerals, provides useful information that has both clinical and public health importance.

Analysis of the PMF-only regions of interest was feasible with QM, and results demonstrated heterogeneity of dust deposition in lung tissue based on particle type. Although the burden of birefringent mineral particles appeared similar within the PMF-only lesion and the adjacent non-PMF tissue, the burden of coal-containing dust was significantly greater within the PMF-only region. Pinkerton et al<sup>18</sup> found that environmental particulate matter deposition in autopsy specimens disproportionately affected respiratory bronchioles.

Additional mineralogic studies of occupationally exposed cohorts could help to characterize histopathologic patterns of lung dust retention.

The moderate correlation ( $r = 0.52$ ) between Mineral: Carbon<sub>[QM]</sub> and Mineral:Carbon<sub>[SEM/EDS]</sub> reflects some variability between these 2 techniques. SEM/EDS identifies particles longer than 0.1  $\mu\text{m}$ , compared with the 0.3- $\mu\text{m}$  threshold for QM. Although SEM/EDS analysis was performed on only 1000 to 2000 particles per sample because of time constraints, QM-PM counts all visible particles over an entire tissue sample, including the more than 100 000 birefringent particles per sample, and all visualized regions of pigmented particulate matter. These technical differences may explain the lack of a strong correlation while highlighting potential benefits of QM-PM.

Our study has a number of strengths. Notably, we had access to lung tissue from a unique cohort of occupationally exposed coal miners with severe disease. These samples had been extensively characterized by both SEM/EDS and an expert international panel of pulmonary pathologists requiring substantial time for consensus agreement on pathology classifications. As such, these tissue samples were ideal for demonstrating the utility and reliability of QM-PM for in situ dust characterization. Normal control lung tissue samples were also evaluated using this technique to provide comparative context for the quantitative particulate matter measurements.

Our study also has several limitations. First, there is no gold standard methodology for in situ lung dust particle characterization. We made general comparisons between QM-PM and existing techniques, but accurate test characteristics (eg, sensitivity and specificity) of this novel approach are impossible to define without a gold standard. Comparisons made in this study are intended to establish general agreement among techniques while highlighting logistical and operational advantages of QM-PM. Second, though QM-PM is unable to provide elemental classification of individual particles, we used existing mineralogy literature informed by findings from SEM/EDS to assess birefringent RCS, other silicates, and pigmented dust. Other birefringent mineral types such as carbonates may exist, but these totaled less than 0.1% of the mineral particles identified using SEM/EDS. Pigmented regions may contain iron oxides or other metallics that would have been differentiated with SEM/EDS. We considered whether the measurement of particle birefringence using QM-PM might be technically limited by small particle size, but further investigation demonstrated the presence of strong birefringence even in the smallest particles (Figure 5). Third, evaluation of birefringent particles under PLM relies heavily on stereologic orientation of particles in cross section. Because of this limitation, birefringent particles were identified and counted, and visible short and long axes were measured; however, these may not fully describe particle shape.

Although QM-PM may eventually assist pathologists, pulmonologists, and occupational medicine specialists in making clinical diagnoses, its greatest value may be as a highly accessible technique for assessing previously unrecognized workplace exposures driving preventable diseases. The utility of QM-PM underscores the value of reactivating and expanding lung tissue databases, such as the National Coal Workers' Autopsy Study or other autopsy programs, for well-characterized worker cohorts. Future investigations may be

helpful in characterizing retained dust in other cohorts with exposure-related lung disease, including the estimated 2 million workers exposed to RCS in the United States<sup>19</sup> and the 60 000 incident cases of pneumoconiosis annually worldwide.<sup>20</sup> Additional efforts to enhance the utility of QM-PM could focus on effectively discerning distinct types of in situ mineral particles based on relative birefringence, including characterizing other birefringent mineral particles (ie, nonsilica and nonsilicates) and assessing additional features that might be used for particle classification.

## CONCLUSIONS

A novel QM-PM method using conventional bright-field microscopy and PLM with image-processing software shows promise in characterizing in situ birefringent lung minerals including RCS and other silicates, as well as carbonaceous particulate matter. Identification of particulate matter using this approach is comparable to existing methods but is substantially less labor-intensive and costly. It is largely automated, is quantitative, and requires little clinical or technical training. In combination with earlier studies,<sup>15,21</sup> our QM-PM findings of increased mineral burden in contemporary coal miners with PMF support ongoing public health interventions focused on silica dust exposure control to address the resurgence of severe lung disease in coal miners, likely from modern mining practices. By enabling consistent and accessible histopathologic screening for exposure-related lung diseases, this novel method may also help inform future efforts aimed at protecting workers in other dusty trades.

## Acknowledgments

This work was funded by grants T42OH009229 (CDC/NIOSH Mountain & Plains Education and Research Center), 2T32HL007085-46 (NIH/NHLBI fellowship training program), the Reuben M. Cherniack fellowship award at National Jewish Health, and FC820-59 (Alpha Foundation for the Improvement of Mine Safety and Health).

The authors would like to thank our occupational pulmonary pathology colleagues Jerrold L. Abraham, MD; Francis H. Y. Green, MD; Jill Murray, MBBCh; and Soma Sanyal, MD, for their previous work classifying the brightfield and polarizing light microscopy specimens used for comparison in this study. We thank Ann F. Hubbs, DVM, PhD, and Marlene S. Orandle, DVM, PhD, at the National Institute for Occupational Safety and Health for their assistance with biopsy specimens. We thank Camille M. Moore, PhD, in the Center for Genes, Environment, and Health at National Jewish Health for her biostatistical assistance.

## References

1. Cohen RA, Rose CS, Go LHT, et al. Pathology and mineralogy demonstrate respirable crystalline silica is a major cause of severe pneumoconiosis in US coal miners. *Ann Am Thorac Soc.* 2022; 19(9):1469–1478. doi:10.1513/AnnalsATS.202109-1064OC [PubMed: 35353671]
2. Almborg KS, Zell-Baran L, Abraham JL, et al. Intra- and inter-rater reliability of pathologic classification of type of progressive massive fibrosis among deceased US coal miners. *Am J Respir Crit Care Med.* 2020;201:A2632. doi: 10.1164/ajrccm-conference.2020.201.1\_MeetingAbstracts.A2632
3. Sarver E, Kele Ç, Afrouz SG. Particle size and mineralogy distributions in respirable dust samples from 25 US underground coal mines. *Int J Coal Geol.* 2021;247:103851. doi:10.1016/j.coal.2021.103851
4. Silicosis and Silicate Disease Committee. Diseases associated with exposure to silica and nonfibrous silicate minerals: Silicosis and Silicate Disease Committee. *Arch Pathol Lab Med.* 1988;112(7):673–720. [PubMed: 2838005]

5. McDonald JW, Roggli VL. Detection of silica particles in lung tissue by polarizing light microscopy. *Arch Pathol Lab Med*. 1995;119(3):242–246. [PubMed: 7887777]
6. Kleinerman J, Green F, Harley R, et al. Pathology standards for coal workers' pneumoconiosis. *Arch Pathol Lab Med*. 1979;103(8):375–432. [PubMed: 378179]
7. Hamilton N. Quantification and its applications in fluorescent microscopy imaging. *Traffic*. 2009;10(8):951–961. doi:10.1111/j.1600-0854.2009.00938.x [PubMed: 19500318]
8. Santa N, Keles C, Saylor JR, Sarver E. Demonstration of optical microscopy and image processing to classify respirable coal mine dust particles. *Minerals*. 2021;11(8):838. doi:10.3390/min11080838
9. Mirsadraee M. Anthracosis of the lungs: etiology, clinical manifestations and diagnosis: a review. *Tanaffos*. 2014;13(4): 1–13. [PubMed: 25852756]
10. Schneider CA, Rasband WS, Eliceiri KW. NIH Image to ImageJ: 25 years of image analysis. *Nat Methods*. 2012;9(7):671–675. doi:10.1038/nmeth.2089 [PubMed: 22930834]
11. Arun Gopinathan P, Kokila G, Jyothi M, Ananjan C, Pradeep L, Humaira Nazir S. Study of collagen birefringence in different grades of oral squamous cell carcinoma using picosirius red and polarized light microscopy. *Scientifica (Cairo)*. 2015;2015:802980. doi:10.1155/2015/802980 [PubMed: 26587310]
12. Lowers H, Breit G, Strand M, et al. Method to characterize inorganic particulates in lung tissue biopsies using field emission scanning electron microscopy. *Toxicol Mech Methods*. 2018;28(7):475–487. doi:10.1080/15376516.2018.1449042 [PubMed: 29685079]
13. Lowers H, Arslan Z. Characteristics of dust associated with the development of rapidly progressive pneumoconiosis and progressive massive fibrosis: US Geological Survey data release. <https://www.sciencebase.gov/catalog/item/628f84d8d34ef70cdba407d2>. Published 2022. Accessed January 12, 2023.
14. Schober P, Boer C, Schwarte LA. Correlation coefficients: appropriate use and interpretation. *Anesth Analg*. 2018;126(5):1763–1768. doi:10.1213/ane.0000000000002864 [PubMed: 29481436]
15. Cohen RA, Petsonk EL, Rose C, et al. Lung pathology in US coal workers with rapidly progressive pneumoconiosis implicates silica and silicates. *Am J Respir Crit Care Med*. 2016;193(6):673–680. doi:10.1164/rccm.201505-1014OC [PubMed: 26513613]
16. Harrison JC, Brower PS, Attfield MD, et al. Surface composition of respirable silica particles in a set of US anthracite and bituminous coal mine dusts. *J Aerosol Sci*. 1997;28:689–696. doi:10.1016/S0021-8502(96)00033-X
17. Wallace WE, Harrison JC, Grayson RL, et al. Aluminosilicate surface contamination of respirable quartz particles from coal mine dusts and from clay works dusts. *Ann Occup Hyg*. 1994;38:439–445. doi:10.1093/annhyg/38.inhaled\_particles\_VII.439
18. Pinkerton K, Green F, Saiki C, et al. Distribution of particulate matter and tissue remodeling in the human lung. *Environ Health Perspect*. 2000;108:1063–1069. doi:10.1289/ehp.001081063 [PubMed: 11102298]
19. OSHA. OSHA FactSheet: OSHA's respirable crystalline silica standard for construction. <https://www.osha.gov/sites/default/files/publications/osh3681.pdf>. Published 2017. Accessed September 10, 2021.
20. Shi P, Xing X, Xi S, et al. Trends in global, regional and national incidence of pneumoconiosis caused by different aetiologies: an analysis from the Global Burden of Disease Study 2017. *Occup Environ Med*. 2020;77(6):407–414. doi: 10.1136/oemed-2019-106321 [PubMed: 32188634]
21. Laney AS, Petsonk EL, Hale JM, Wolfe AL, Attfield MD. Potential determinants of coal workers' pneumoconiosis, advanced pneumoconiosis, and progressive massive fibrosis among underground coal miners in the United States, 2005–2009. *Am J Public Health*. 2012;102(suppl 2):S279–S283. doi:10.2105/AJPH.2011 [PubMed: 22401526]

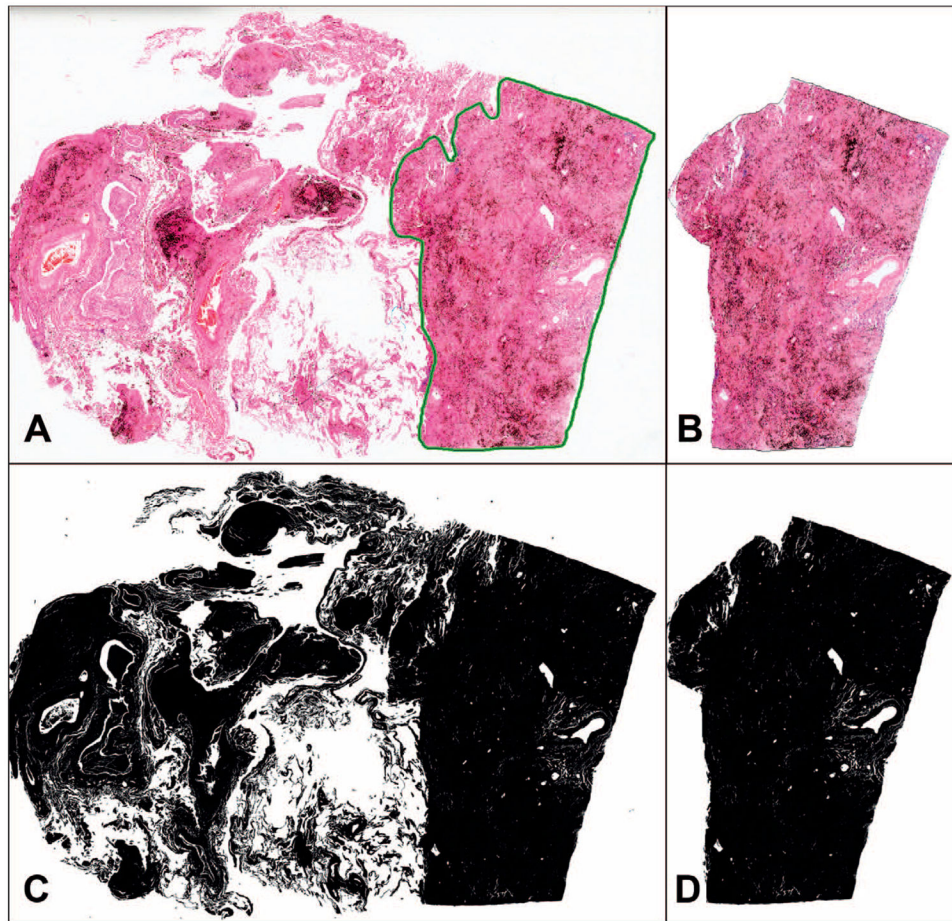


**Figure 1.** Automated tissue area and area of interest identification. A, Hematoxylin and eosin–stained slide with pathologist demarcation of a progressive massive fibrosis (PMF) lesion (green line). B, Segmentation of PMF tissue lesion. C, Binary image of total tissue area selected based on grayscale brightness threshold using ImageJ software. D, Binary image of PMF lesion alone using ImageJ (original magnification  $\times 2$  [A through D]).

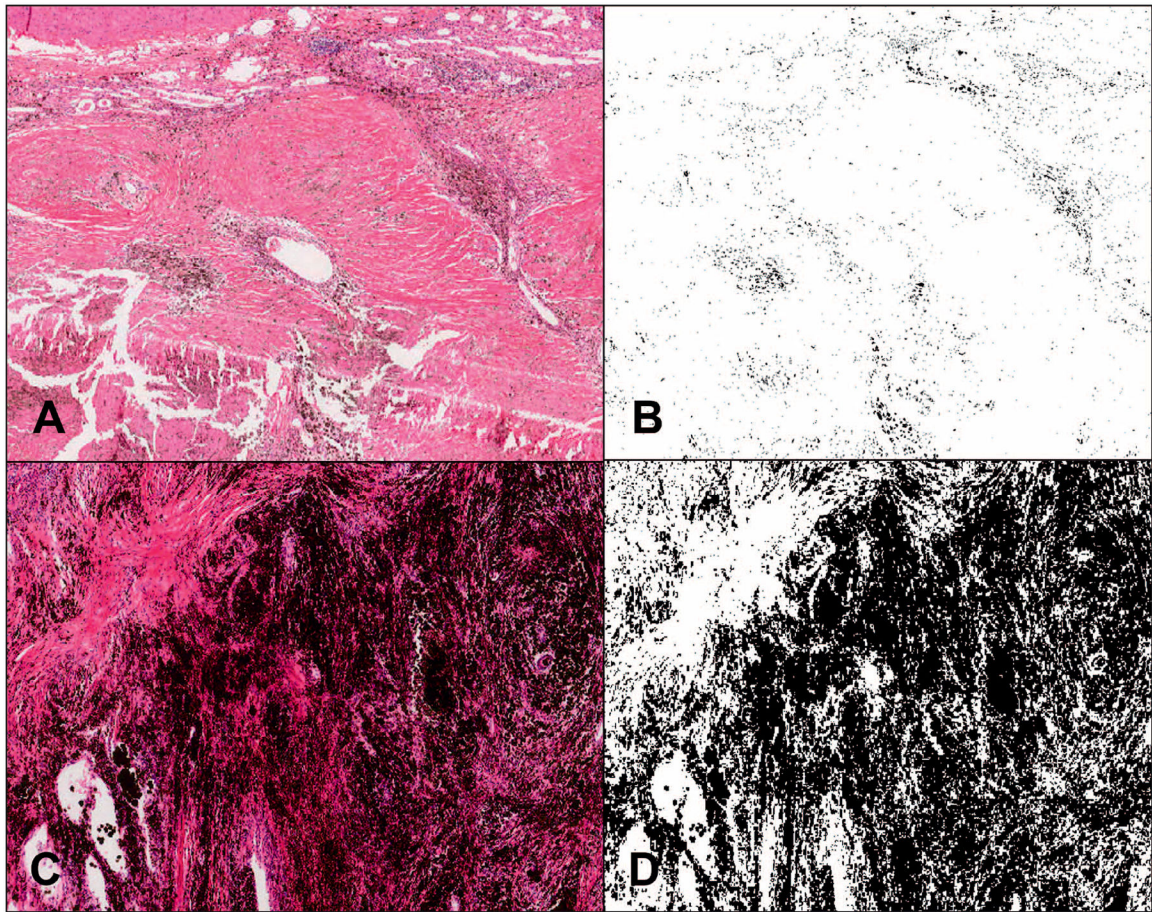


**Figure 2.** Automated pigment (coal/carbonaceous) identification. Hematoxylin and eosin–stained slide with corresponding binary image showing automated detection of brown/black pigmented regions using ImageJ. This example shows a low pigment burden (A and B) and a high pigment burden (C and D) (original magnification  $\times 4$  [A through D]).

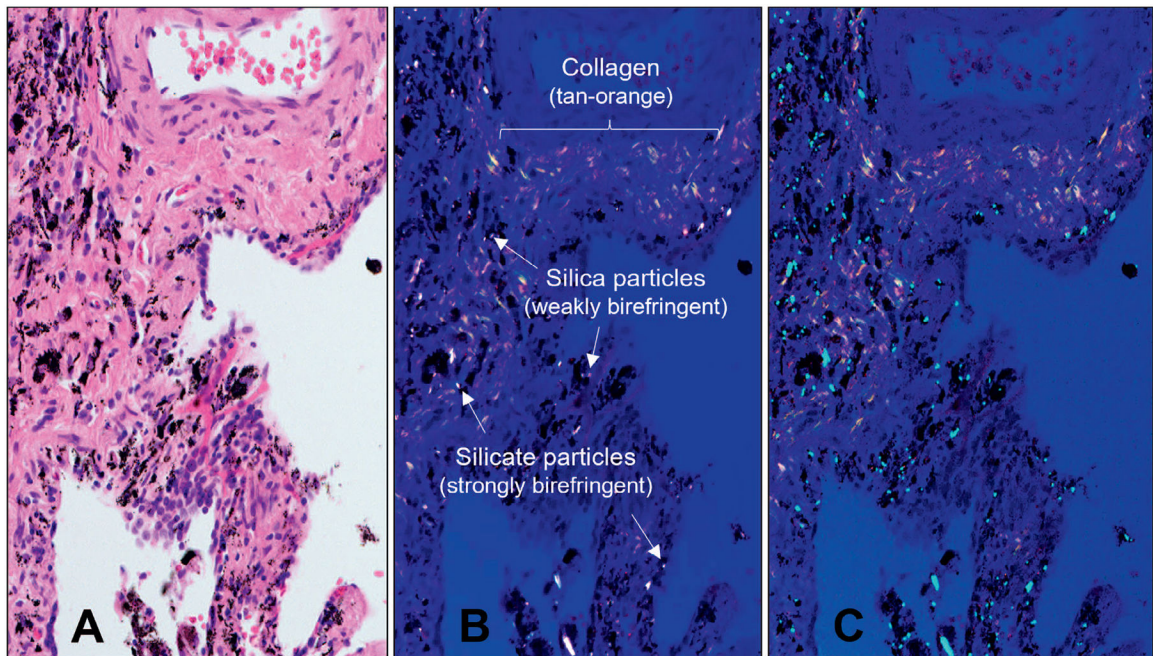


**Figure 3.** Automated birefringent mineral identification using modified built-in Keyence BZ-X800 series microscopy software with the Macro Hybrid Cell Count feature. Single hematoxylin and eosin–stained slide section viewed using bright-field microscopy (A); polarized light microscopy (PLM) highlighting silica, silicates, and collagen fibers (B); and PLM with teal-blue overlay showing automated identification of birefringent mineral particles while avoiding collagen (C) (original magnification  $\times 20$  [A through C]).

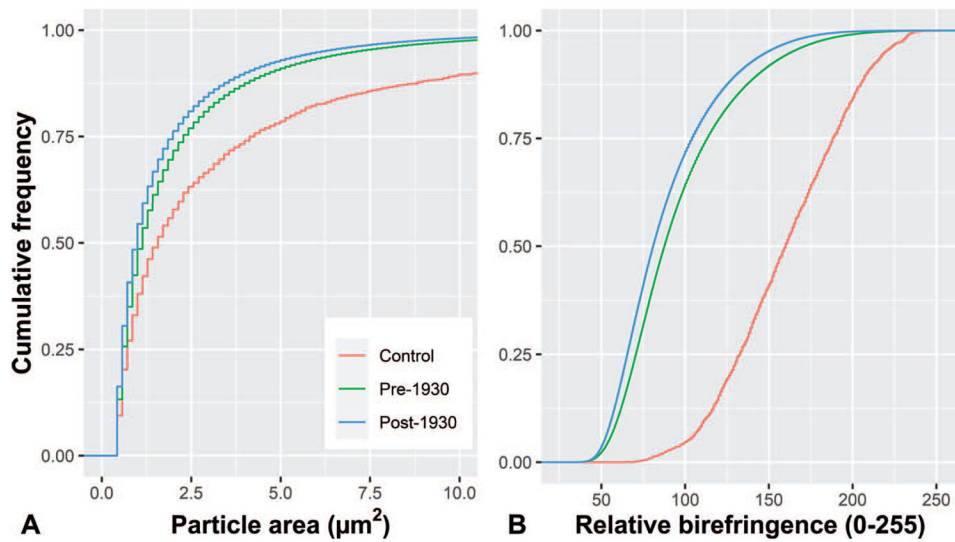


**Figure 4.** Particle-level characteristics for birefringent mineral particles identified using quantitative microscopy–particulate matter for normal controls (red), historical coal miners (green), and contemporary coal miners (blue). Cumulative frequency of particles based on (A) particle area ( $\mu\text{m}^2$ ) and (B) mean particle grayscale brightness under polarized light (range, 0 [black]–255 [white]; higher value indicates stronger birefringence). Mineral particles in contemporary and historical miners were similar in size and brightness, but both had smaller particles and weaker birefringence (less bright) than controls ( $P < .05$ ).

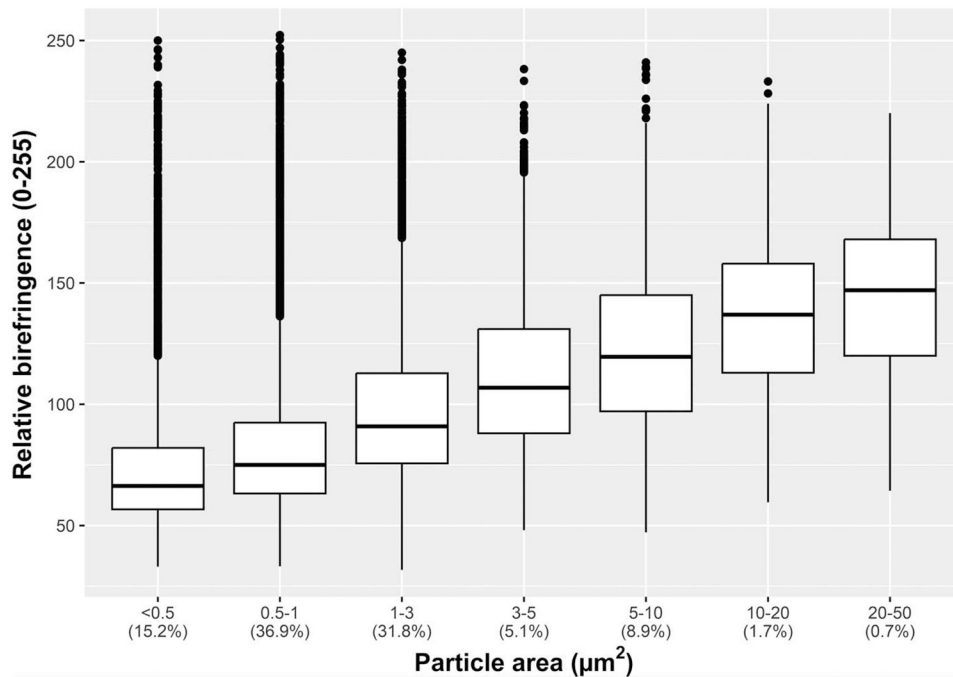


**Figure 5.**

Mean particle birefringence (grayscale brightness range, 0 [black]–255 [white]) of mineral particles identified using quantitative microscopy–particulate matter (QM-PM) grouped by particle size. Notably, strong birefringence (brightness values closer to 255) was observed even in the smallest mineral particles ( $<0.5 \mu\text{m}^2$ ), suggesting that the ability for minerals such as silicates to appear bright on QM-PM is not technically limited by small size. The particles represented in this figure are a random selection totaling 1% (for ease of graphical visualization) of the 9 670 264 birefringent mineral particles analyzed from all samples in this study.

Demographics of Controls and US Coal Miners With Progressive Massive Fibrosis (PMF) Characterized by Pathologist Consensus

Table 1.

|  | Controls<br>(n = 10) | Coal Miners With PMF<br>(n = 85) | Miner Birth Cohort <sup>a</sup> |                       |
|--|----------------------|----------------------------------|---------------------------------|-----------------------|
|  |                      |                                  | Historical (n = 62)             | Contemporary (n = 23) |
| Age, mean (range), y   | 52.7 (17–71)         | 64.2 (48–82)                     | 65.4 (55–82)                    | 61.1 (48–79)          |
| Male, No. (%)  | 5 (50)               | 85 (100)                         | 62 (100)                        | 23 (100)              |
| Current or former smoker, No. (%)  | 3/6 (50)             | 67 (79)                          | 50 (81)                         | 17 (74)               |
| Smoking pack-years, mean (SD)  | 12.2 (16.1)          | 19.6 (18.7)                      | 20.1 (19)                       | 18.6 (18.4)           |
| Years of coal mining, mean (SD)  | ...                  | 34.9 (8.4)                       | 35.8 (10)                       | 31.4 (2.2)            |
| Years of underground coal mining, mean (SD)                              | ...                  | 33.8 (8.2)                       | 34.9 (8.9)                      | 30.2 (8.7)            |
| Work in central Appalachian state, No. (%) <sup>b</sup>                  | ...                  | 56 (66)                          | 39 (63)                         | 17 (74)               |
| Pathologist-determined PMF type, No. <sup>c</sup>                        |                      |                                  |                                 |                       |
| Coal   | ...                  | 35                               | 31                              | 4                     |
| Mixed  | ...                  | 26                               | 20                              | 6                     |
| Silica   | ...                  | 24                               | 11                              | 13                    |
| Pathologist-determined birefringent particle profusion, No. <sup>d</sup> |                      |                                  |                                 |                       |
| Mild   | ...                  | 28                               | 21                              | 7                     |
| Moderate   | ...                  | 40                               | 30                              | 10                    |
| Severe   | ...                  | 17                               | 11                              | 6                     |

<sup>a</sup>Historical miners defined as birth year prior to 1930; contemporary miners defined as birth in 1930 or later. Additional demographic information for coal miners is detailed in Cohen et al.<sup>1</sup>

<sup>b</sup>Central Appalachian state refers to the states of Kentucky, Virginia, and West Virginia.

<sup>c</sup>Type of PMF: 25% of the PMF lesion containing silicotic nodules, coal type; >75% containing silicotic nodules, silica type; and >25% and 75% containing silicotic nodules, mixed type.

<sup>d</sup>Birefringent particle profusion (qualitative) defined by pathologist assessment based on visual appearance under polarized light microscopy as either mild, moderate, or severe.

**Table 2.** Birefringent Particle Characteristics Using Quantitative Microscopy for Controls and US Coal Miners With Progressive Massive Fibrosis

|  | Controls<br>(n = 10) | All Miners<br>(n = 85) | Miner Birth Cohort <sup>b</sup> |                        |                          | Qualitative Birefringent Particle Profusion <sup>c</sup> |                      |                    |                      |
|--|----------------------|------------------------|---------------------------------|------------------------|--------------------------|--|----------------------|--------------------|----------------------|
|  |                      |                        | P Value <sup>a</sup>            | Historical<br>(n = 62) | Contemporary<br>(n = 23) | Mild<br>(n = 28)   | Moderate<br>(n = 40) | Severe<br>(n = 17) | P Value <sup>d</sup> |
| Sample-level birefringent mineral characteristics, mean (SD)         |                      |                        |                                 |                        |                          |  |                      |                    |                      |
| Mineral particles identified/sample                                  | 210 (158)            | 113 284 (186 678)      | ...                             | 64 763 (59 341)        | 244 079 (314,284)        | 39 430 (58 217)  | 113 698 (167 093)    | 233 949 (290 111)  | ...                  |
| Tissue volume (mm <sup>3</sup> )                                     | 0.06 (0.02)          | 1.07 (0.38)            | ...                             | 1.01 (0.34)            | 1.24 (0.44)              | 0.95 (0.36)  | 1.17 (0.39)          | 1.04 (0.32)        | ...                  |
| Mineral density, particles/mm <sup>3</sup>                           | 4542 (4543)          | 96 936 (140 008)       | <.001                           | 63 727 (55 318)        | 186 456 (234 253)        | 37 372 (42 259)  | 91 865 (111 806)     | 206 976 (224 253)  | <.001                |
| Mineral:Carbon[QM]   | 0.19 (0.32)          | 0.49 (0.92)            | .04                             | 0.23 (0.35)            | 1.21 (1.48)              | 0.23 (0.73)  | 0.45 (0.75)          | 1.3 (1.33)         | <.001                |
| Individual birefringent particle-level characteristics, median (IQR) |                      |                        |                                 |                        |                          |  |                      |                    |                      |
| Particle area, <i>d</i> μm <sup>2</sup>                              | 1.57 (0.71–4.20)     | 1.00 (0.57–2.14)       | <.001                           | 1.14 (0.57–2.28)       | 1.00 (0.57–1.99)         | 1.0 (0.57–2.28)  | 0.99 (0.57–1.99)     | 1.14 (0.57–2.28)   | .67                  |
| Particle short-axis dimension, μm                                    | 0.82 (0.51–1.58)     | 0.64 (0.38–1.07)       | <.001                           | 0.68 (0.48–1.13)       | 0.60 (0.38–1.05)         | 0.68 (0.42–1.07)   | 0.60 (0.36–1.01)     | 0.68 (0.48–1.13)   | .83                  |
| Particle long-axis dimension, μm                                     | 1.69 (0.84–3.38)     | 1.19 (0.84–2.03)       | <.001                           | 1.20 (0.85–2.14)       | 1.20 (0.85–1.89)         | 1.19 (0.84–2.03)   | 1.19 (0.76–1.89)     | 1.19 (0.84–2.03)   | .61                  |
| Particle grayscale brightness <sup>e</sup>                           | 160.0 (133.0–188.0)  | 83.7 (67.4–108)        | <.001                           | 87.6 (70.6–113.2)      | 80.9 (65.5–104.1)        | 89.0 (72.5–113.5)  | 81.3 (64.8–107.0)    | 84.5 (69.0–107.3)  | .23                  |

Abbreviations: IQR, interquartile range (25th to 75th percentile); Mineral:Carbon[QM], ratio of the cumulative birefringent particle area in square micrometers to the pigmented (carbonaceous) area in square micrometers using quantitative microscopy; mineral density, number of birefringent mineral particles measured using quantitative microscopy per cubic millimeter of tissue.

<sup>a</sup>One-way analysis of variance or 2-tailed *t* test for group-level comparison of continuous variables. Post-hoc Tukey tests for multiple pairwise comparisons of mineral density and Mineral:Carbon[QM] were all significant (*P* < .05). Comparisons of birefringent particle-level characteristics were performed with linear mixed models using groups as fixed effects and samples as random effects. Mineral density, Mineral:Carbon[QM], and particle size characteristics were log transformed prior to test statistic calculation.

<sup>b</sup>Historical miners defined as birth year prior to 1930; contemporary miners defined as birth in 1930 or later.

<sup>c</sup>Pathologist birefringent particle profusion classification for miners based on qualitative visual appearance of birefringent particulate matter using polarized light microscopy by pathologist groups with consensus agreement.

<sup>d</sup>Particle area represents the 2-dimensional surface area of individual particles identified using quantitative microscopy.

<sup>e</sup>Mean grayscale brightness of individual birefringent mineral particles (range, 0 [black]–255 [white]) under polarized light microscopy. Greater values represent stronger birefringence.